Chemistry and Physics of Lipids 222 (2019) 51–58

Contents lists available at ScienceDirect

Chemistry and Physics of Lipids

journal homepage: www.elsevier.com/locate/chemphyslip

Lipodisqs for eukaryote lipidomics with retention of viability: Sensitivity and resistance to *Leucobacter* infection linked to *C.elegans* cuticle composition

Juan F. Bada Juarez, Delia O'Rourke, Peter J. Judge, Li C. Liu, Jonathan Hodgkin*, Anthony Watts*

Department of Biochemistry, University of Oxford, South Parks Road, OX1 3QU, Oxford, United Kingdom

ARTICLE INFO

Keywords:
Lipodisq
SMALP
SMA
Lipid nanoparticle
C. elegans
agmo-1
Lipidomics
AGMO
MALDI-MS
Ether lipid
Leucobacter
Verde1
Verde2
Cuticle
Lipid
Styrene-maleic acid polymer
Detergent-free
Alkylglycerol monooxygenase
Bacterial infection

ABSTRACT

Lipodisq™ nanoparticles have been used to extract surface lipids from the cuticle of two strains (wild type, N2 and the bacteria-resistant strain, *agmo-1*) of the *C. elegans* nematode without loss of viability. The extracted lipids were characterized by thin layer chromatography and MALDI-TOF-MS. The lipid profiles differed between the two strains. The extracted lipids from the bacteria-resistant strain, *agmo-1*, contained ether-linked (O-alkyl chain) lipids, in contrast to the wild-type strain which contained exclusively ester- linked (O-acyl) lipids. This observation is consistent with the loss of a functional alkylglycerol monooxygenase (AGMO) in the bacterial resistant strain *agmo-1*. The presence and abundance of other lipid species also differs between the wild-type N2 and *agmo-1* nematodes, suggesting that the *agmo-1* mutant strain attempts to compensate for the increase in ether-linked lipids by modulating other lipid-synthesis pathways. Together these differences not only affect the fragility of the cuticle and the buoyancy of the worm in aqueous buffer, but also interactions with surface-adhering bacteria. The much greater chemical stability of O-alkyl, non-hydrolysable linked lipids compared with hydrolysable O-acyl linked lipids, may be the origin of the resistance of the *agmo-1* strain to bacterial infection, providing a more resilient cuticle for the nematode. Additionally, we show that lipid extraction with a polymer of styrene and maleic acid (SMA) provides a viable route to lipidomics studies with minimal perturbation of the organism.

1. Introduction

C. elegans has been a successful model organism for the study of both animal development and behaviour for more than 50 years (Sulston and Hodgkin, 1988; Brenner, 1974). The genome was the first from a multicellular organism to be sequenced (Bloom, 1998) and their simplicity makes them a perfect system for studies of gene expression, ageing, development and the nervous system (Riddle et al., 1997). The *C. elegans* "exoskeleton" (Page, 2007), the cuticle, which forms a barrier between the external environment and the worm epidermis, is poorly characterized. The cuticle has an important role in *C. elegans* biology, as it maintains body shape while permitting locomotion and nutrition, and also offers protection against bacterial and fungal parasites (Blaxter, 1993).

Previously, we described the isolation of two new *Leucobacter* bacterial pathogens of *Caenorhabditis*, discovered co-infecting a wild isolate collected in Cape Verde (Hodgkin et al., 2013). The interactions of these bacteria with *C. elegans* revealed unusual mechanisms of pathogenic attack: one pathogen, Verde1, traps swimming nematodes by sticking their tails together, resulting in the formation of "worm-star" aggregates, in which worms were killed and degraded; the other pathogen, Verde2, kills worms by a different mechanism associated with rectal infection. Both infections require the attachment of bacteria to the cuticle for their pathogenic effects (Hodgkin et al., 2013).

Genetic screens identified many distinct mutant worms that were resistant to lethal *Leucobacter* Verde2 infection. The mutations alter the chemical properties of the worm surface, preventing Verde2 attachment and also affecting movement, sensitivity to bleach and the binding of

* Corresponding authors.
E-mail addresses: athan.hodgkin@bioch.ox.ac.uk (J. Hodgkin), anthony.watts@bioch.ox.ac.uk (A. Watts).

https://doi.org/10.1016/j.chemphyslip.2019.02.005
Received 30 October 2018; Received in revised form 19 February 2019; Accepted 20 February 2019
Available online 15 May 2019

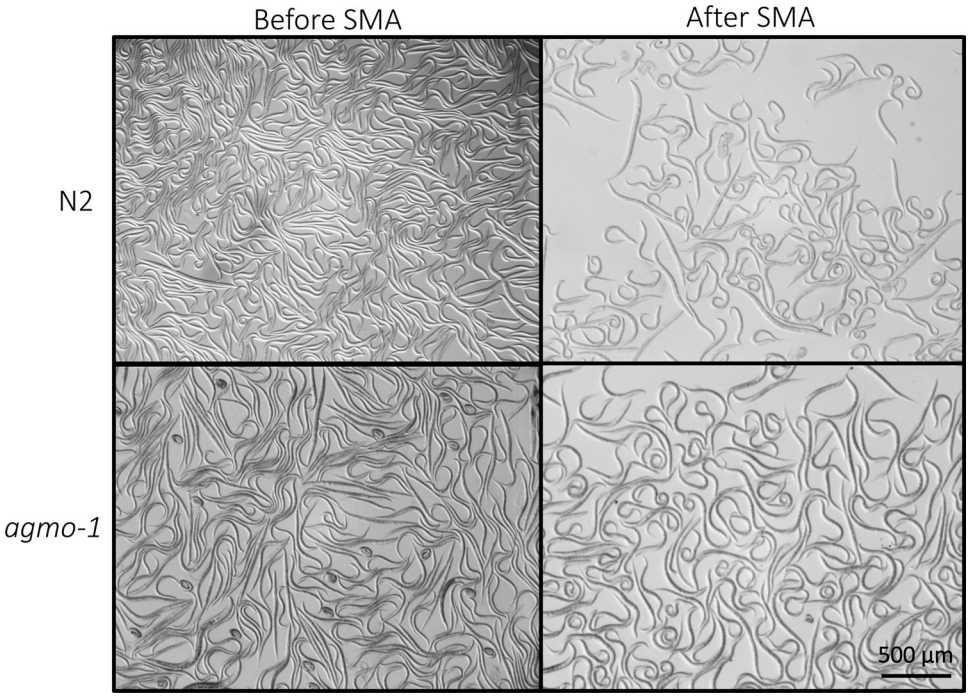

Fig. 1. *C. elegans* wild-type (N2) and mutant (agmo-1) worms, imaged here both before (left) and after (right) addition of SMA polymer. The worms were grown on nematode growth plates and generations were synchronised the L2/L3 larval stages to provide homogenous populations (Brenner, 1974). *C. elegans* nematodes were imaged using a Leica MZFLIII microscope and Hamamatsu digital camera (Orca-05 G), equipped with HCImage software (Hamamatsu). The viability and integrity of the worms were not affected as shown here.

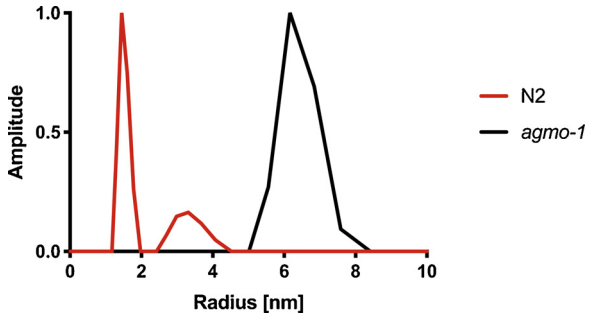

Fig. 2. Dynamic light scattering experiment showing the different particle sizes obtained following SMA addition to each of the two *C. elegans* strains. Radii were measured using a Malvern Zetasiser Nano S instrument. Data were processed using Malvern Zetasizer software.

Table 1
DLS data for the SMA nanoparticles from the wild-type (N2) and the mutant strain (agmo-1).

Peak (radius)	N2	*agmo-1*
SMA polymer	1.5 ± 0.1 nm	–
Lipodisq nanoparticles	3.3 ± 0.4 nm	6.4 ± 0.4 nm

lectins. The Verde2-resistant mutants are however hypersensitive to *Leucobacter* Verde1 infection. Further genetic suppressor screens to reverse the lethal sensitivity of these mutants to Verde1 suggested a common mechanism involved in suppression of Verde1 infection, identified as the loss of the pathway required for the degradation of ether lipids. Many independent suppressor mutations were found in the gene encoding alkylglycerol monooxygenase (AGMO), a metabolic enzyme solely responsible for the degradation of ether-linked lipids (Watschinger and Werner, 2013; Loer et al., 2015), or in enzymes required for the synthesis of its essential cofactor tetrahydrobiopterin (Watschinger and Werner, 2013; Watschinger et al., 2015). This striking reciprocal sensitivity and resistance to Verde1 and Verde2 may reflect the fact that these pathogens were isolated as a co-infection of wild-type *Caenorhabditis*, suggesting that the worms may have developed a trade-off relationship between sensitivity and resistance to the two pathogens (Hodgkin et al., 2013).

The finding that loss of the ether lipid degradation pathway confers resilience to Verde1 infection, suggests that changes in the lipid content of the *C. elegans* cuticle are responsible for altering the susceptibility to the Verde1 and Verde2 infection mechanisms (Hodgkin et al., 2013). Here we complement the genetic analysis of *C. elegans* surface with a biochemical analysis of the cuticle lipidome, both in mutants that demonstrate resistance to Verde1 infection and in wild-type worms.

The *C. elegans* cuticle is secreted by the underlying epithelial cells and is regenerated entirely following moulting at four larval growth stages (L1-4). It is thought that the thickness of the cuticle, as well as its protein and lipid composition, change at every larval stage and may vary in response to the environment (Riddle et al., 1997; Page, 2007). The cuticle consists of several layers, the outermost being the surface coat, which is covered by glycoproteins and has a net negative charge at neutral pH, due to the presence of sugar-sulphate moieties (Blaxter, 1993). This outermost layer is likely to play an important role in locomotion and may prevent the adhesion of microbes to the nematode surface (Page, 2007). *C. elegans srf* mutants, with an altered carbohydrate epitope expression profile on the coat, have a weakened cuticle and modified bacterial adherence (Page, 2007). Other additional *bus* (Bacterially UnSwollen) mutants show similar phenotypes, including modified surface lectin binding (Gravato-Nobre et al., 2005).

Below the hydrophilic surface coat, the epicuticle contains both glycoproteins and lipids, including non-polar species such as steroids (particularly cholesterol), polar lipids such as PC and PE and some glycolipids, which appear to have important roles in the immune response (Blaxter, 1993; Chisholm and Xu, 2012). With the exception of the epicuticle and the surface coat, the cuticle is predominantly made of collagen and its derivatives (cross-linked and collagen-like molecules) (Johnstone, 1994). The epicuticle of the parasitic nematode *Trichinella spiralis*, is mainly composed of PC, PE and PG and has lipids arranged in an inside-out cylindrical configuration, in which the hydrophilic headgroups point inwards, exposing the hydrophobic tails to the rest of the cuticle (Gounaris et al., 1996).

Lipid mobility in the cuticles of several nematode species is restricted compared to a typical plasma membrane (Riddle et al., 1997; Kusel et al., 1991). The presence of lipids in the epicuticle of other

Table 2
Thin layer chromatography (TLC) was performed using silica gel plates and a mobile phase of methanol:chloroform:ammonium hydroxide (65:25:4 v/v/v). The different lipids present (with their retention factors in brackets) were identified by comparison to literature values. ND denotes unidentified lipids.

N2	*agmo-1*	N2 from Blaxter, 1993
PE (0.79)	PMME (0.71)	PI (0.09)
LPG (0.54)	CL (0.67)	ND (0.24)
SM (0.28)	PG (0.6)	PC (0.38)
LPS (0.18)	–	PE (0.5)
CE (1)		ND (0.61)
Cb (0.94)		Sterol (0.9)
LPC (0.22)		ND (1)

Full name	Abbreviation
Glycerophosphocholines	PC (LPC for lyso species)
Glycerophosphoethanolamines	PE (LPE for lyso species)
Glycerophosphoserines	PS (LPS for lyso species)
Glycerophosphoglycerols	PG (LPG for lyso species)
Glycerophosphates	PA (LPA for lyso species)
Glycerophosphoinositols	PI (LPI for lyso species)
Glycerophosphoglycerophosphoglycerols (Cardiolipins)	CL
Monoradylglycerolipids	MG
Diradylglycerolipids	DG
Triradylglycerolipids	TG
Digalactosyldiacylgylcerols	DGDG
Sulfoquinovosyldiacylglycerols	SQDG
Ceramides/Sphingoid bases	Cer/Sph
Hexosyl ceramides	HexCer
Mannosyl-PI-ceramides	MIPC
Mannosyl-di-PI-ceramides	$M(IP)_2C$
Lactosyl ceramides	LacCer
Sulfatides	SHexCer
Wax esters	WE
Cholesteryl esters	CE
Fatty acids	FA
Lyso-phosphatidylinositol-monophosphate	LPIP

nematodes has been assessed by fluorescent probes and lipase treatment (Riddle et al., 1997; Page, 2007; Witting and Schmitt-Kopplin, 2016; Lee, 2002) and the flexibility and resistance to chemical and physical stresses have been attributed to the presence of some waxes and/or glycolipids (ascarosides (Lee, 2002)). Conversely, proteins in the epicuticle have been shown to diffuse quickly, which is attributed both to weak ionic interactions with lipids and also due to their distribution in membrane domains containing neutral lipids, in which they can diffuse freely (Riddle et al., 1997; Kusel et al., 1991).

We set out to identify the components of the nematode surface in order to understand how defects in lipid metabolism change the surface of *C. elegans* and thereby alter patterns of bacterial adherence. We focused on differences between wild-type N2 worms and the most frequently identified Verde1 suppressor mutant, *agmo-1*, which lacks alkylglycerol monooxygenase (AGMO) (Watschinger and Werner, 2013; Loer et al., 2015). By disrupting the metabolic pathways responsible for lipid synthesis (Loer et al., 2015), loss of the enzyme might alter the sensitivity towards bacterial pathogens through a destabilization of the cuticle. While the total lipidome of *C. elegans* has been partially analysed using imaging, genetic and biochemical techniques (Witting and Schmitt-Kopplin, 2016; Matyash et al., 2008; Zhang and Hou, 2013; Shi et al., 2016), the characterization the of *C. elegans* surface has been limited (Blaxter, 1993), owing to the difficulty of selectively extracting lipids from the cuticle, without contamination from other cellular membranes in the worm.

SMA (a hydrolysed co-polymer of styrene and maleic anhydride) has recently been shown to be able to simultaneously extract both lipids and proteins from biological membranes. The polymer extracts lipids non-selectively, preserving protein structure and activity (Scheidelaar et al., 2015; Esmaili and Overduin, 2018; Dominguez Pardo et al., 2017; Xue et al., 2018). The resulting nanoparticles (commonly termed Lipodisq or SMALPs) have also been used for structural characterization by cryo-EM (Parmar et al., 2018; Sun et al., 2018; Qiu et al., 2018) and X-ray crystallography (Broecker et al., 2017). Several membrane proteins including ion channels (Dörr et al., 2014) and GPCRs (Jamshad et al., 2015; Logez et al., 2016) have been studied and characterized from different organisms (Gulati et al., 2014; Postis et al., 2015; Swainsbury et al., 2018; Long et al., 2013) and some proteomics and lipidomics experiments have been performed using SMALPs by hydrogen-deuterium exchange mass spectrometry and LC–MS/MS (Reading, 2018; Reading et al., 2017; Teo et al., 2019). The interactions between lipids and two further novel amphipathic polymers (a copolymer of Diisobutylene/Maleic Acid (commonly known as DIBMA) and poly(methacrylate) (commonly known as PMA)), both of which lack the styrene groups present in SMA, have recently been characterised and their behaviour suggests that they may also be suitable for lipid extraction for similar lipidomics studies (Oluwole et al., 2017; Yasuhara et al., 2017).

Here, SMA polymer is used to extract the lipids present in the nematode cuticle of *C. elegans* wild-type (N2) and *agmo-1* strains. We characterise the surface lipids from the wild-type and mutant strains of *C. elegans* using MALDI-TOF-MS. Our aim is to identify and understand the molecular differences in cuticle composition and structure, which underpin the different phenotypes of the wild-type and surface-mutant nematodes.

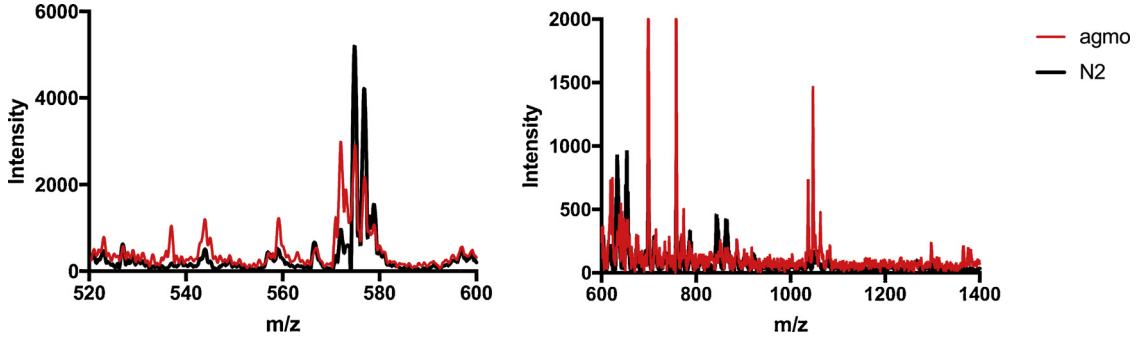

Fig. 3. MALDI-MS spectra at different *m/z* ranges exhibiting different peaks. In red the agmo-1 mutant and in dark the wild-type. Some differences are observed especially in the 600–1200 m/z region. Lipid extracts were spotted onto an MTP 384 Polished Steel TF target and MALDI-MS spectra were acquired using a Bruker Ultraflex TOF/TOF spectrometer operating in linear positive ion mode.

Table 3
The different lipids identified in SMA extracts using the LipidMAPS database (Sud et al., 2007). In red the lipids which have been identified as ether-linked lipids (with O- indicating alkyl ether-linked lipids and P-indicating alkneyl-ether (plasmalogen) lipids) and in green lipids which are shared between the wild-type and mutant strain. In orange, the different ceramides with d and t designating the shorthand notation for sphingolipids and referring to 1,3-dihydroxy and 1,3,4-trihydroxy long-chain bases.

agmo-1				
Mass (Da)	**Abbreviation**	**Full name**	**Headgroup net charge**	**Chain length and unsaturation**
1539.587	TG	Triradylglycerolipid	0	99:0
1385.993	DGDG	Digalactosyldiacylglycerol	0	65:7
1369.024	PIP	Glycerophosphoinositol monophosphate	-2	65:1
1366.886	CL or PIP	Cardiolipin or Glycerophosphoinositol monophosphate	-2	66:7 or 66:8
1290.895	PIP	Glycerophosphoinositol monophosphate	-2	60:5
1279.758	PIP	Glycerophosphoinositol monophosphate	-2	58:7
1277.554	$M(IP)_2C$	Mannosyl-di-glycerophosphoinositol-ceramide	-2	d46:3
1165.738	SQDG	Sulfoquinovosyldiacylglycerol	-1	57:9
1158.823	PE	Glycerophosphoethanolamine	0	64:10
1148.848	LacCer	Lactosyl ceramide	0	t50:0
1141.55	$M(IP)_2C$	Mannosyl-di-PI-ceramide	-2	d31:2
1134.746	PC	Glycerophosphocholine	0	58:12
1120.828	PC or PE	Glycerophosphocholine or Glycerophosphoethanolamine	0	58:8 or 61:8
1107.787	PS	Glycerophosphoserine	-1	60:10
1106.841	LacCer	Lactosyl ceramide	0	d50:2
1087.602	PIP	Glycerophosphoinositol monophosphate	-2	46:8
1006.738	DGDG	Digalactosyldiacylglycerol	0	39:1
947.71	PA, PG or TG	Glycerophosphoglycerol	-1	O-53:6, P-50:6, 58:11
946.785	TG	Triradylglycerolipid	0	58:9
888.844	DG or TG(O) or TG(P)	Diacylglycerol or Triacylglycerol	0	54:3, O-54:3, P-54:2
850.358	PIP	Glycerophosphoinositol monophosphate	-2	27:2
837.42	SQDG	Sulfoquinovosyldiacylglycerols	-1	33:5
824.388	LPIP	Lyso-Glycerophosphoinositol monophosphate	-2	25:1
811.422	LPIP	Lyso-Glycerophosphoinositol monophosphate	-2	29:3
760.465	ShexCer	Sulfatides hexosyl ceramide	-1	d31:1
751.324	SQDG	Sulfoquinovosyldiacylglycerol	-1	27:6
703.549	HexCer	Hexosylceramide	0	t32:2
698.689	CE or WE	Ceramide or Wax ester	0	20:0 or 47:5
655.376	PA	Glycerophosphate	-1	30:2
653.3	SQDG	Sulfoquinovosyldiacylglycerol	-1	24:6
603.446	PI	Glycerophosphoinositol	-1	57:0
576.466	PG	Glycerophosphoglycerol	-1	62:4
566.379	PI	Glycerophosphoinositol	-1	55:9

(*continued on next page*)

Table 3 (*continued*)

N2				
Mass (Da)	Abbreviation	Full name	Headgroup net charge	Chain length and unsaturation
996.704	PS	Glycerophosphoserine	-1	48:1
811.422	LPIP	Lyso-Glycerophosphoinositol monophosphate	-2	29:3
760.332	MIPC	Mannosyl-PI-ceramide	-1	t18:0
655.376	PA	Glycerophosphate	-1	30:2
653.3	SQDG	Sulfoquinovosyldiacylglycerol	-1	24:6
566.379	PI	Glycerophosphoinositol	-1	55:9

2. Material and methods

2.1. C. elegans culture

The N2 (wild-type) and *agmo-1* (strain CB7014, genotype *agmo-1(e3016)*) nematodes were grown on nematode growth media plates (Brenner, 1974). The generations were synchronized in order to obtain a homogeneous population prior to SMA polymer addition.

2.2. Formation of Lipodisq nanoparticles

SMA polymer containing a molar ratio of styrene:maleic acid of 3:1 was supplied by Malvern Cosmeceutics Ltd (Malvern, UK). Synchronised populations of worms were harvested by washing the media plates with 10 mM Tris 5 mM NaCl pH 8 followed by three rounds of centrifugation (2500*g*, 2 min, 4 °C). An SMA solution (25% w/v in 50 mM Tris buffer pH 8) was added to the washed worms at a final concentration of 12.5% v/v in 50 mM Tris buffer pH 8 and incubated for 30 min at 30–40 °C. The sample was centrifuged, and the supernatant was kept for further analysis.

2.3. Dynamic light scattering measurements

The size of the Lipodisq nanoparticles, generated by lipid extraction by SMA, was measured by Dynamic Light Scattering at 633 nm using a Malvern Zetasizer Nano S instrument with a disposable cuvette. Data were processed using Malvern Zetasizer software.

2.4. Viability test of worms after SMA treatment

Worms were deposited onto a freshly seeded OP50 NGM plate and left at room temperature. The recovery was assessed from the percentage of worms that crawled across the OP50 making visible tracks. Plates were observed under a dissecting microscope after 1, 2, 4 and 24 h, and were compared to those with nematodes that had not been exposed to SMA.

2.5. Lipids extraction from Lipodisq nanoparticles

Lipids were extracted from the Lipodisq samples according to the method of Bligh and Dyer (1959). Briefly, 200 µL Lipodisq-containing sample was mixed vigorously for 1 h, with 2 mL chloroform/methanol (2:1 v/v). Phase separation was achieved by adding 1 mL of ddH_2O water. The extract was left for 10 min at room temperature and then centrifuged (1,000*g*, 10 min) and the lower phase was retrieved washed twice with a methanol/water mix (1:1 v/v) and dried under a stream of N_2 gas.

2.6. Matrix-assisted laser desorption ionization mass spectrometry

Water and DHB matrix were spotted onto a MALDI plate (MTP 384 Polished Steel TF Targets) and allowed to dry at room temperature. Lipids were resuspended in chloroform/methanol mixture (2:1 v/v), deposited above the dried matrix and allowed to dry at room temperature. MALDI TOF mass spectra were acquired using a Bruker Ultraflex TOF/TOF operating in linear positive ion mode. MALDI laser intensity was selected to provide optimal intensity and resolution of acquired mass spectra. External calibration was performed using protein standards and some lipids standards, which were analysed under identical conditions. The identification of lipid was performed using LIPID MAPS online searching tools (Sud et al., 2007) and data analysis was performed using the Thermo XCalibur (ThermoFisher) processing software and plotted in Prism (GraphPad software).

3. Results

To determine the cuticle lipid composition of both wild-type (N2) and mutant (*agmo-1*) *C. elegans*, nematodes were incubated with SMA polymer. Both the time of incubation and temperature were adjusted to ensure that both wild-type and mutant worms recovered after the SMA treatment as shown in Fig. 1. The best conditions for the SMA extraction of the nematode surface were found to be a temperature of between 30 °C and 40 °C and an incubation time of 30–60 minutes.

After incubation, the SMA-worm suspension was centrifuged, the supernatant was collected and DLS measurements were performed to verify Lipodisq nanoparticle formation (Fig. 2; Table 1). DLS data show that Lipodisqs were present in the supernatant (peak at 4–6 nm), although some excess SMA was still present in the N2 strain sample (identified by the peak at 1.3 nm). The *agmo-1* mutant strain did not contain any excess SMA, despite the fact that the same number of worms was used to perform this experiment as for the wild type. A viability test showed that more than 95% of the worms survived the SMA incubation (data not shown).

After the DLS analysis, the lipid composition of the Lipodisq nanoparticles from both nematode strains were investigated. Lipids were extracted by following the method of Bligh and Dyer (1959) and were analysed by thin layer chromatography (TLC) (Fig. SI.1), as described previously (Dörr et al., 2014; Reading, 2018). Lipid headgroups were identified by their retention factor (R_f) values (Table 2). Ceramides, commonly found in the skin of mammals (Pappas, 2009) in which they appear to play a role in the organisation of other lipids (Bouwstra et al., 1998), are found in both wild-type and mutant worms, and their appearance is consistent with the slow lipid diffusion rates previously reported in the cuticle (Riddle et al., 1997; Kusel et al., 1991; Hou and Taubert, 2012). Also present in both strains were cerebrosides (Cb) and lyso-phosphatidylcholine (LPC). For the N2 strain, lipids such as phosphoethanolamine (PE), lyso-phosphatydilglycerol (LPG), sphingosine/sphingomyelin (SM) and lyso-phosphatydilserine (LPS) were found, whereas in the mutant *agmo-1*, phosphatidyl-N-monomethylethanolamine (PMME), cardiolipin (CL) and PG were found. Also, some lipid species are not able to migrate in the chosen solvent mixture, and this might indicate the presence of highly charged species as speculated by Blaxter and colleagues (Blaxter, 1993).

TLC is not able to distinguish between ester- and ether-linked lipids with the same headgroup and MALDI-TOF MS was therefore used to assist in the identification of some of the lipids present. As some of these lipids have a mass below 1 kDa, the instrument was calibrated using low molecular weight protein standards in addition to lipids such as DMPC, POPC, DOPC and POPG. Moreover, as the 500 Da–1000 Da mass range is difficult to study due to the noise peaks produced by the matrix, a control experiment including the recording of mass spectra of matrix-only spots was performed (data not shown) and the peaks of this matrix-only experiment were subtracted from the Lipodisq sample experiments. Another control was performed which includes the removal of the peaks coming the OP50 bacterial source lipids extracted using SMA. Matrix-only peaks were subtracted from the mass spectra of N2 and *agmo-1*. The mass spectra for the N2 and *agmo-1* after removal of both the matrix and OP50 lipids peaks are shown in Fig. 3.

Lipid peaks were determined with an intensity above 500 (signal-to-noise ratio > 20) and peaks were assigned (Table 3). Identification of lipids was performed using the LipidMAPS database (Sud et al., 2007) with a mass tolerance of ± 0.1 *m/z*. All peaks were considered as possible ion adducts with potassium, sodium, with a possible loss of water and as singly and doubly charged, (MALDI primarily generates sodium and potassium adducts of singly or doubly charged species (Abonnenc et al., 2010)). As expected, no ether lipids (coloured red in Table 3), were identified in the N2 wild-type strain, however up to two ether lipid species were identified in the *agmo-1* mutant.

Some lipid species (rendered in green in Table 3) are observed in both the N2 and *agmo-1* samples, including PA, PI, sulfoquinovosyldiacylglycerol (SQDG) and lyso-phosphatidylinositol-monophosphate (LPIP). In addition to these lipids, the N2 strain has some additional lipid types which include PS and MIPC.

4. Discussion

The SMA lipid extraction method used here, appears to be milder than protocols involving detergent or organic extractions (Blaxter, 1993), and the fact that 95% of the nematodes are viable after treatment with SMA, suggests that the integrity of the cell membranes in the *C. elegans* body is not severely compromised, and that the polymer primarily extracts lipids from the cuticle.

The DLS data suggest that the lipid extraction from the worms by SMA, results in the formation of Lipodisq nanoparticles, with diameters measured in the range 6–13 nm (Table 1), similar to those previously reported (Dörr et al., 2016; Esmaili and Overduin, 2018; Lee et al., 2016; Orwick et al., 2012; Orwick-Rydmark et al., 2012). The sizes of the particles formed, differs between the N2 and *agmo-1* strains, consistent with a difference in lipid content and also might indicate differences in protein content. Additionally, the N2 cuticle is more resistant to SMA treatment, in agreement with earlier studies which indicate that the *agmo-1* cuticle is more fragile (Loer et al., 2015). The accumulation of ether lipids may compromise the stability of the *agmo-1* cuticle, despite its ability to prevent *Leucobacter* Verde1 attachment to the *C. elegans* surface.

Identification of lipid headgroups was carried by TLC and some retention factors measured in previous publications (Blaxter, 1993) are similar to our data and can be identified (TLC solvent systems, 2019). Therefore, the $R_f = 0.24$ could be LPC-type lipids and the $R_f = 0.61$, could be PG-type lipids. Some of the lipids found in the Lipodisq extraction were also identified by Blaxter and colleagues, such as PE and ceramides, however we were unable to identify PC or PI from in our data (Table 2). The presence of SQDG and ceramide-type lipids (Fig. 3 and Table 3) is consistent with literature, especially for the sulfonated lipids, which are responsible for the negative charge on the cuticle. All of the lipids identified by the TLC analysis are lipid species expected from previous genetic studies of *C. elegans* (Witting and Schmitt-Kopplin, 2016).

Since the *agmo-1* mutant lacks alkylglycerol monooxygenase (AGMO), which cleaves the ether bond of alkylglycerols, we expect to observe some differences in the abundance of ether-linked lipids in the mutant. Compared to the wild-type strain, more lipids were observed and identified for the *agmo-1* mutant, as seen by the TLC (Fig. SI. 1). The lipids highlighted (in red in Table 3) are ether-linked lipid species, which have been speculated to accumulate at the cuticle surface due to the lack of the AGMO enzyme. Previous studies suggest that sulfatides, PE and PI have the lowest detectability threshold (Fuchs et al., 2010) and their identification in this experiment, may mean that the sample contains a high amount of these lipids (which is not surprising as PI and sulfatides lipids have been suggested to regulate the cuticle surface charge (Blaxter, 1993)).

The accumulation of some ether-linked lipids at the cuticle surface of the mutant, may prevent bacterial adherence by masking binding targets on the worm surface. The *agmo-1* nematodes float on aqueous buffer (unlike wild-type worms) consistent with an increased abundance of ether-linked lipids and waxes, both of which have been reported to affect buoyancy (Magnusson and Haraldsson, 2011). The wild-type cuticle also contains greater relative abundance of negatively charged lipid headgroups, which are diluted by the ether-linked lipids and ceramides in the *agmo-1* mutant, which may also explain the differences in the apparent ease of solubilisation of the cuticle lipids by the negatively charged SMA polymer.

Surprisingly we also observe some ester-linked lipid species in the *agmo-1* mutant which are not found in the N2 strain. We propose that a compensation mechanism is effected, which results in the upregulation of other lipid synthesis pathways and the more heterogeneous lipid

composition of the mutant cuticle. A similar phenomenon has been observed in murine macrophage-like cells, in which a decrease in AGMO activity (and increase in free alkylglycerol lipid types) resulted in widespread alterations in the cell lipidome, including changes in the abundance of glycosylated ceramides and cardiolipin10. In our case, we found several glucosyl-ceramides in the *agmo-1* mutant, which have been suggested to be located in the nematode cuticle (Kage-Nakadai et al., 2010), some tri- and diacylglycerols and only one cardiolipin (Watschinger et al., 2015). We suggest that the protein composition also differs as a result of changes in lipid-protein interactions.

Ether lipid-deficient strains in *C. elegans* accumulate high levels of stearic acid (18:0) in several types of ester-linked lipid, presumably to compensate for the reduced rigidity that would be conferred by the ether lipids (Watts and Ristow, 2017). It is striking that longer chain length lipids with high molecular weights are observed in the *agmo-1* mutant but not the N2 strain. The wild-type cuticle has a less diverse lipidome, and the lipids present generally have shorter acyl chain lengths than the mutant.

5. Conclusion

We have demonstrated that lipid extraction by SMA may be used to study the lipidome of the *C. elegans* cuticle. We have shown that SMA can be used on living organisms without affecting their viability, compared to harsher lipid extraction methods such as those requiring organic solvents (Fig. 1). We have identified an accumulation of ether-linked lipids in the *agmo-1* mutant nematode cuticle, which is consistent with the deletion of a functional alkylglycerol monooxygenase (AGMO) in this strain (Loer et al., 2015). The presence and abundance of other lipid species also differ between the wild-type N2 and *agmo-1* worms, suggesting that the mutant strain attempts to compensate for the increase in ether-linked lipids by modulating other lipid-synthesis pathways. Together these differences not only affect the fragility of the cuticle (Loer et al., 2015) and the buoyancy of the worm in aqueous buffer, but also the interactions between the exoskeleton and surface-adhering bacteria (Loer et al., 2015).

Acknowledgments

We thank Dr Holger Kramer for access to MS equipment and Peter Fisher for technical assistance. This study was partly funded by MRC grant MR/J001309/1 and a Faucett Catalyst Grant (to JH). We also thank Malvern Cosmeceutics (Steve Tonge and Andy Harper) for their continued support and supply of SMA polymer.

Appendix A. Supplementary data

Supplementary material related to this article can be found, in the online version, at doi:https://doi.org/10.1016/j.chemphyslip.2019.02.005.

References

Abonnenc, M., Qiao, L., Liu, B., Girault, H.H., 2010. Electrochemical aspects of electrospray and laser desorption/Ionization for mass spectrometry. Annu. Rev. Anal. Chem. Palo Alto Calif (Palo Alto Calif) 3, 231–254.
Blaxter, M.L., 1993. Cuticle surface proteins of wild type and mutant Caenorhabditis elegans. J. Biol. Chem. 268, 6600–6609.
Bligh, E., Dyer, W., 1959. Canadian journal of biochemistry and physiology. J. Biochem. Physiol. 37, 911–917.
Bloom, F.E., 1998. Staying afloat on the seas of data. *Science* 80, 282 1989.
Bouwstra, J.A., et al., 1998. Role of ceramide 1 in the molecular organization of the stratum corneum lipids. J. Lipid Res. 39, 186–196.
Brenner, S., 1974. The genetics of Caenorhabditis elegans. Genetics. https://doi.org/10.1002/cbic.200300625.
Broecker, J., Eger, B.T., Ernst, O.P., 2017. Crystallogenesis of membrane proteins mediated by polymer-bounded lipid nanodiscs. Structure 25, 384–392.
Chisholm, A.D., Xu, S., 2012. The Caenorhabditis elegansepidermis as a model skin. II: differentiation and physiological roles. Wiley Interdiscip. Rev. Dev. Biol. 1, 879–902.
Dominguez Pardo, J.J., et al., 2017. Solubilization of lipids and lipid phases by the styrene–maleic acid copolymer. Eur. Biophys. J. 46, 91–101.
Dörr, J.M., et al., 2014. Detergent-free isolation, characterization, and functional reconstitution of a tetrameric K^+ channel: the power of native nanodiscs. Proc. Natl. Acad. Sci. 111, 18607–18612.
Dörr, J.M., et al., 2016. The styrene–maleic acid copolymer: a versatile tool in membrane research. Eur. Biophys. J. 45, 3–21.
Esmaili, M., Overduin, M., 2018. Membrane biology visualized in nanometer-sized discs formed by styrene maleic acid polymers. Biochim. Biophys. Acta Biomembr. 1860, 257–263.
Fuchs, B., Süß, R., Schiller, J., 2010. An update of MALDI-TOF mass spectrometry in lipid research. Prog. Lipid Res. 49, 450–475.
Gounaris, K., Smith, V.P., Selkirk, M.E., 1996. Structural organisation and lipid composition of the epicuticular accessory layer of infective larvae of Trichinella spiralis. Biochim. Biophys. Acta Biomembr. 1281, 91–100.
Gravato-Nobre, M.J., et al., 2005. Multiple genes affect sensitivity of Caenorhabditis elegans to the bacterial pathogen Microbacterium nematophilum. Genetics 171, 1033–1045.
Gulati, S., et al., 2014. Detergent-free purification of ABC (ATP-binding-cassette) transporters. Biochem. J. 461, 269–278.
Hodgkin, J., Félix, M.-A., Clark, L.C., Stroud, D., Gravato-Nobre, M.J., 2013. Two Leucobacter strains exert complementary virulence on Caenorhabditis Including death by worm-star formation. Curr. Biol. 23, 2157–2161.
Hou, N.S., Taubert, S., 2012. Function and regulation of lipid biology in Caenorhabditis elegans aging. *Front. Physiol.* 3 (May), 1–10.
Jamshad, M., et al., 2015. G-protein coupled receptor solubilization and purification for biophysical analysis and functional studies, in the total absence of detergent. Biosci. Rep. 35, 1–10.
Johnstone, I.L., 1994. The cuticle of the nematode Caenorhabditis elegans: a complex collagen structure. BioEssays 16, 171–178.
Kage-Nakadai, E., et al., 2010. Two very long chain fatty acid acyl-CoA synthetase genes, acs-20 and acs-22, have roles in the cuticle surface barrier in Caenorhabditis elegans. PLoS One 5.
Kusel Jr., L.P., S. H. V & W, K. M, 1991. Biophysical Properties of the Nematode Surface. *Parasit. Nematodes—Membranes, Antigens Genes*.
Lee, D.L., 2002. The Biology of the Nematodes. CRC Press.
Lee, S.C., et al., 2016. A method for detergent-free isolation of membrane proteins in their local lipid environment. Nat. Protoc. 11, 1149–1162.
Loer, C.M., et al., 2015. Cuticle integrity and biogenic amine synthesis in Caenorhabditis elegans require the cofactor tetrahydrobiopterin (BH4). Genetics 200, 237–253.
Logez, C., et al., 2016. Detergent-free isolation of functional g protein-coupled receptors into nanometric lipid particles. Biochemistry 55, 38–48.
Long, A.R., et al., 2013. A detergent-free strategy for the reconstitution of active enzyme complexes from native biological membranes into nanoscale discs. BMC Biotechnol. 13, 41.
Magnusson, C.D., Haraldsson, G.G., 2011. Ether lipids. Chem. Phys. Lipids 164, 315–340.
Matyash, V., Liebisch, G., Kurzchalia, T.V., Shevchenko, A., Schwudke, D., 2008. Lipid extraction by methyl- *tert* -butyl ether for high-throughput lipidomics. J. Lipid Res. 49, 1137–1146.
Oluwole, A.O., et al., 2017. Solubilization of membrane proteins into functional lipid-bilayer nanodiscs using a Diisobutylene/Maleic acid copolymer. Angew. Chemie - Int. Ed. 56, 1919–1924.
Orwick, M.C., et al., 2012. Detergent-free formation and physicochemical characterization of nanosized lipid-polymer complexes: lipodisq. Angew. Chemie - Int. Ed. 51, 4653–4657.
Orwick-Rydmark, M., et al., 2012. Detergent-free incorporation of a seven-transmembrane receptor protein into nanosized bilayer lipodisq particles for functional and biophysical studies. Nano Lett. 12, 4687–4692.
Page, A., 2007. The cuticle. WormBook 1–15. https://doi.org/10.1895/wormbook.1.138.1.
Pappas, A., 2009. Epidermal surface lipids. Dermatoendocrinol. 1, 72–76.
Parmar, M., et al., 2018. Using a SMALP platform to determine a sub-nm single particle cryo-EM membrane protein structure. Biochim. Biophys. Acta Biomembr. 1860, 378–383.
Postis, V., Rawson, S., Mitchell, J., 2015. The use of SMALPs as a novel membrane protein scaffold for structure study by negative stain electron microscopy. Biochim. Biophys. Acta - Biomembr. 1848, 496–501.
Qiu, W., et al., 2018. Structure and activity of lipid bilayer within a membrane-protein transporter. Proc. Natl. Acad. Sci. 115, 201812526.
Reading, E., 2018. Structural mass spectrometry of membrane proteins within their native lipid environments. Chem. - A Eur. J. https://doi.org/10.1002/chem.201801556.
Reading, E., et al., 2017. Interrogating membrane protein conformational dynamics within native lipid compositions. Angew. Chemie - Int. Ed. 56, 15654–15657.
Riddle, D.L., Blumenthal, T., Meyer, B.J., 1997. C. Elegans. Cold Spring Harbor.
Scheidelaar, S., et al., 2015. Molecular Model for the solubilization of membranes into nanodisks by styrene maleic acid copolymers. Biophys. J. 108, 279–290.
Shi, S., Luke, C.J., Miedel, M.T., Silverman, G.A., Kleyman, T.R., 2016. Activation of the caenorhabditis elegans degenerin channel by shear stress requires the MEC-10 subunit. J. Biol. Chem. 291, 14012–14022.
Sud, M., et al., 2007. LMSD: LIPID MAPS structure database. Nucleic Acids Res. 35, 527–532.
Sulston, J., Hodgkin, J., 1988. *The nematode Caenorhabditis elegans*. Cold Spring Harbor Lab.
Sun, C., et al., 2018. Structure of the alternative complex III in a supercomplex with cytochrome oxidase. Nature 557, 123–126.
Swainsbury, D.J.K., et al., 2018. Probing the local lipid environment of the Rhodobacter

sphaeroides cytochrome bc1and Synechocystis sp. PCC 6803 cytochrome b6f complexes with styrene maleic acid. *Biochim. Biophys. Acta - Bioenerg* 1859, 215–225.
Teo, A.C.K., et al., 2019. Analysis of SMALP co-extracted phospholipids shows distinct membrane environments for three classes of bacterial membrane protein. Sci. Rep. 9, 1813.
Watschinger, K., Werner, E.R., 2013. Alkylglycerol monooxygenase. IUBMB Life 65, 366–372.
Watschinger, K., et al., 2015. Tetrahydrobiopterin and alkylglycerol monooxygenase substantially alter the murine macrophage lipidome. Proc. Natl. Acad. Sci. 112, 2431–2436.
Watts, J.L., Ristow, M., 2017. Lipid and carbohydrate metabolism in Caenorhabditis elegans. Genetics 207, 413–446.
Witting, M., Schmitt-Kopplin, P., 2016. The Caenorhabditis elegans lipidome: a primer for lipid analysis in Caenorhabditis elegans. Arch. Biochem. Biophys. 589, 27–37.
Xue, M., Cheng, L., Faustino, I., Guo, W., Marrink, S.J., 2018. Molecular mechanism of lipid nanodisk formation by styrene-maleic acid copolymers. Biophys. J. 115, 494–502.
Yasuhara, K., et al., 2017. Spontaneous lipid nanodisc fomation by amphiphilic polymethacrylate copolymers. J. Am. Chem. Soc. 139, 18657–18663.
Zhang, R., Hou, A., 2013. Host-Microbe interactions in Caenorhabditis elegans. ISRN Microbiol. 2013, 1–7.
TLC solvent systems, TLC solvent systems. Available at: https://avantilipids.com/tech-support/analytical-procedures/tlc-solvent-systems/.